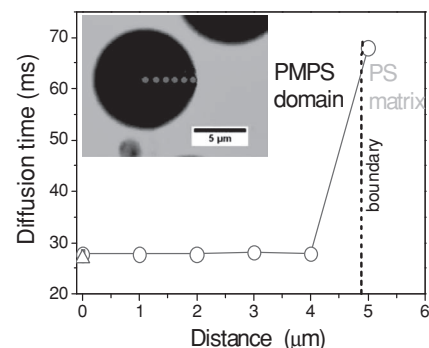


# Monitoring the Dynamics of Phase Separation in a Polymer Blend by Confocal Imaging and Fluorescence Correlation Spectroscopy

Mikheil Doroshenko, Maria Gonzales, Andreas Best, Hans-Jürgen Butt, Kaloian Koynov,\* George Floudas\*

The phase separation of the polymer blend polystyrene/poly(methyl phenyl siloxane) (PS/PMPS) is studied in situ by laser scanning confocal microscopy (LSCM) and by fluorescence correlation spectroscopy (FCS) at macroscopic and microscopic length scales, respectively. It is shown for the first time that FCS when combined with LSCM can provide independent information on the local concentration within the phase-separated domains as well as the interfacial width.



## 1. Introduction

Laser scanning confocal microscopy (LSCM) has emerged as a powerful tool in studying the morphology of heterogeneous systems. For example, LSCM has been extensively used in cell biology<sup>[1]</sup> including the characterization of pharmaceutical systems.<sup>[2]</sup> LSCM is a nondestructive method and has strong depth discrimination that is achieved by proper use of a confocal pinhole in the image plane. In such configuration, only light coming from the

focal point is detected and out-of-focus light is rejected thus the images are practically optical sections. As a result, image processing allows for a 3D visualization of the exact morphology. With respect to the latter, earlier efforts provided with the 3D image of bicontinuous polymer blends obtained via spinodal decomposition.<sup>[3–8]</sup> Subsequent studies tested the calculated structure factor against the measured one via scattering experiments and found an excellent agreement.<sup>[4,5]</sup> Further the LSCM studies in polymer blends include the in situ monitoring of the shrinkage during the photopolymerization process,<sup>[9]</sup> the blend surface morphology,<sup>[10]</sup> the phase separation, and gelation in gelatin/maltodextrin mixtures<sup>[11,12]</sup> and the protein–polymer colocalization in a phase-separated polymer blend.<sup>[13]</sup>

Phase separation via spinodal decomposition<sup>[14–18]</sup> is a widespread phenomenon occurring in diverse systems: from metallic alloys to glasses, ceramics, fluid mixtures, surfactant micellar solutions, and in polymer mixtures. The latter are considered as model systems in studying the phase separation kinetics. Polymers have

M. Doroshenko, M. Gonzales, A. Best, Dr. H.-J. Butt,  
Dr. K. Koynov, Dr. G. Floudas

Max-Planck-Institut für Polymerforschung,  
55021 Mainz, Germany

E-mail: koynov@mpip-mainz.mpg.de; gfloudas@cc.uoi.gr

Dr. G. Floudas

Department of Physics, University of Ioannina, P.O. Box 1186, 45110  
Ioannina, Greece and Foundation for Research and Technology-  
Hellas (FORTH), Biomedical Research Institute (BRI)

long characteristic times that allow studying in situ their morphology during spinodal decomposition. Ideally, one would like to explore the details of the phase separation process in situ by monitoring droplet nucleation, dissolution, approach of droplets, coalescence, and growth within the different regimes. In addition, microscopic information on the interfacial width and of the local composition within the domains is essential.

It is the aim of the present investigation to provide independent information on the local concentration within the phase-separated domains of a polymer blend by combining LSCM with fluorescence correlation spectroscopy (FCS). To our knowledge, this idea has not been explored before. FCS is a powerful tool for monitoring the diffusion of fluorescent molecules, macromolecules, or nanoparticles in various environments.<sup>[19]</sup> With respect to macromolecules, it has been employed earlier in studying the diffusion of small fluorescent tracers in bulk homopolymers with different chain topologies such as linear and star polyisoprenes,<sup>[20]</sup> in polydimethyl siloxane,<sup>[21,22]</sup> poly(*n*-butyl acrylate),<sup>[23]</sup> in miscible polymer blends of 1,4-*cis*-polyisoprene with poly(vinyl ethylene)<sup>[21]</sup> as well as to follow the polymerization process.<sup>[24]</sup> It was shown that the diffusion coefficient of the tracer depends strongly on the glass temperature of the studied systems and as such it can be employed as a reporter for changes in the local polymer dynamics.

The chosen system is a polystyrene/poly(methyl phenyl siloxane) (PS/PMPS) blend. The blend separates upon lowering the temperature, thus exhibits an upper critical solution temperature (UCST). In addition, it possesses large dynamic asymmetry as revealed by the difference between the component glass temperatures,  $\Delta T_g \approx 113$  K at  $P = 0.1$  MPa. The phase behavior has been investigated experimentally and theoretically both at ambient pressure<sup>[25,26]</sup> and more recently at elevated pressures.<sup>[27]</sup> In addition, the glass temperature,  $T_g$ , of the hard phase (PS), interferes with the demixing process thus giving rise to pinning of the domain structure at a certain stage.

## 2. Experimental Section

### 2.1. Materials and Processes

Direct visualization of the phase separation in the PS/PMPS blends using LSCM requires fluorescent labeling of one of the polymers. Fluorescein-labeled polystyrenes with different molecular weights, PS<sub>116</sub> ( $\bar{M}_w = 12.2$  kg mol<sup>-1</sup>) and PS<sub>21</sub> ( $\bar{M}_w = 2.2$  kg mol<sup>-1</sup>), where the subscript in PS<sub>x</sub> denotes the degree of polymerization, were purchased from Polymer Standards Service (PSS, Mainz, Germany) and were further purified via precipitation in methanol to remove any remaining not covalently attached fluorescein molecules. After purification, the samples were characterized by gel permeation chromatography (PS was used as a

■ Table 1. Molecular characteristics of the homopolymers.

$\bar{M}_w, \text{PS}$ [g mol <sup>-1</sup> ]	$N_{\text{PS}}$	$\bar{M}_w/\bar{M}_n$ (PS)	$\bar{M}_w, \text{PMPS}$ [g mol <sup>-1</sup> ]	$N_{\text{PMPS}}$	$\bar{M}_w/\bar{M}_n$ (PMPS)
12200	116	1.17	2270	16	1.67
2230	21	1.20			

standard, THF as an eluent) that yielded molecular weights and polydispersities that are shown in Table 1. PMPS<sub>16</sub> with molecular weight  $\bar{M}_w = 2.27$  kg mol<sup>-1</sup> was synthesized in house following synthesis and purification strategies described previously.<sup>[28]</sup>

Thin films of symmetric PS/PMPS blends (50/50) on microscope cover glasses were prepared as follows. First, 0.02 g of PS and 0.02 g of PMPS were dissolved in 1 g of toluene and the mixture was stirred for 7–8 h at room temperature. Films were prepared by casting the blended solution on round microscope cover glasses with diameter of 25 mm and thickness of 0.15 mm. Although the thickness of the film should be relatively high to minimize surface effects on morphology, most of toluene was evaporated prior casting. The casted films were dried at ambient condition overnight and for further 48 h in vacuum at 50 °C. To follow the phase separation kinetics different specimens from the same blend were annealed under vacuum at various temperatures (from 60 to 140 °C) and for various times (from 30 min up to 24 h) and then quenched to ambient temperature and studied by LSCM.

For the FCS studies, films containing a terylene dye, N,N'-bis(2,6-diisopropylphenyl)-1,6,9,14-tetraphenoxy-terrylene-3,4,11,12-tetra-carboxidiimide (TDI)<sup>[29,30]</sup> were prepared by adding an appropriate amount of a 10<sup>-8</sup> M toluene solution of the dye to the polymer mixture. Experimental details on LSCM and FCS are provided in Supporting Information.

## 3. Results and Discussion

### 3.1. Phase Diagram and Phase Separation by LSCM

The phase diagram of the studied PS<sub>116</sub>/PMPS<sub>16</sub> blend is shown in Figure 1. The diagram is based on model calculations using a lattice-based equation of state that account for the effects of compressibility and nonrandom mixing (details in ref.<sup>[31]</sup>). A recent detailed description on how to implement the theory for polymer blends is available in ref.<sup>[32]</sup>. We mention here that the PS/PMPS theoretical phase diagram was successfully tested earlier against experimental data for different symmetric PS/PMPS blends.<sup>[27]</sup> The type of morphology in polymer blends (spherical or fibrillar dispersed phase vs co-continuous phases), depends not only on the volume fraction but also on the viscosity and elasticity of the components as well as processing conditions.<sup>[14–17,33]</sup>

The symmetric PS<sub>116</sub>/PMPS<sub>16</sub> blend shows clear signs of phase separation. Figure 1 shows a series of the LSCM images from different specimens of the blend that were annealed at 120 °C for different time intervals. In all

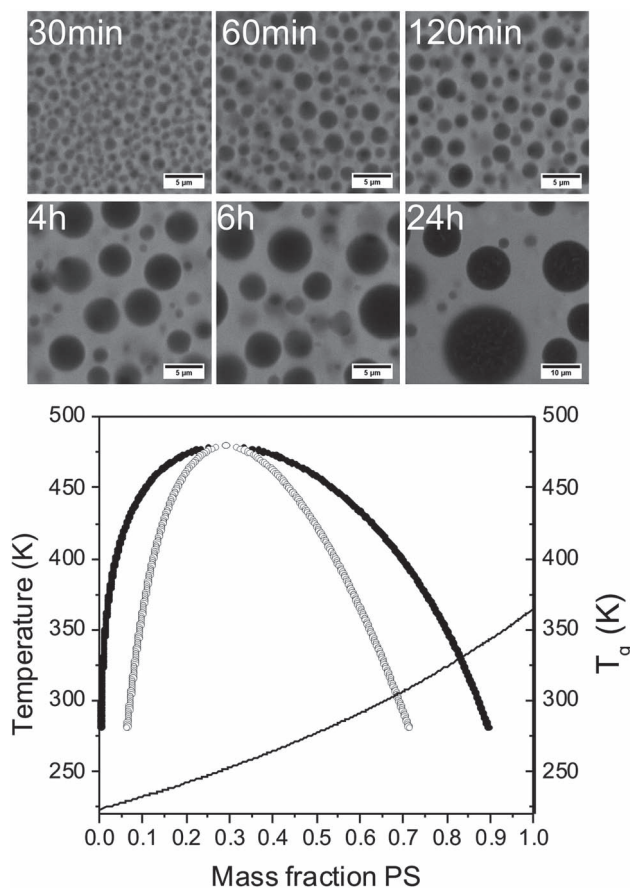


**Figure 1.** (Top) Confocal fluorescence microscopy images showing the effect of annealing time on phase separation of the PS<sub>116</sub>/PMPS<sub>16</sub> blend. Annealing was made at 120 °C and the corresponding annealing time is given in left upper corners. The green area corresponds to fluorescein labeled PS-rich regions, and the dark regions to the unlabeled PMPS-rich regions. The scale bar corresponds to 5 μm except of the bottom right image where it corresponds to 10 μm. (Bottom) Model phase diagram corresponding to the experimental PS<sub>116</sub>/PMPS<sub>16</sub> blend. Both the bimodal (filled symbols) and the spinodal (open symbols) curves are shown. The solid line is the theoretical Fox equation.

images, the green and black domains correspond to PS- and PMPS-rich domains, respectively. At 120 °C, the symmetric blend is located within the two-phase region and is well above the glass temperature of a PS homopolymer with the same degree of polymerization as the PS in the blend ( $T_g^{\text{PS}} = 92$  °C).<sup>[34]</sup> Following this annealing procedure, all specimens were quenched to ambient temperature and imaged. At this temperature the PS-domains are glassy thus restricting any domain growth. For the shortest annealing time ( $t = 30$  min), the morphology consists of a broad distribution of dark spherical domains of the PMPS-rich phase embedded in a continuous PS-rich matrix. With increasing annealing time, the larger PMPS-rich domains grow at the expense of smaller ones and the final distribution resembles more to a bimodal distribution. In addition,

the final annealing temperature has a strong effect on the domain growth. The PMPS-rich domains become larger with increasing annealing temperature that indicates a diffusion controlled process (Figure S2, Supporting Information). The dark domains grow even when annealed at 90 °C, that is, few degrees below the glass temperature of bulk PS. This suggests that the PS matrix includes some fraction of PMPS (i.e. faster) chains. Indeed, earlier dielectric relaxation experiments<sup>[27]</sup> on the symmetric blend PS<sub>48</sub>/PMPS<sub>17</sub> revealed a PS-rich phase with PS composition of volume fraction  $\phi_{\text{PS}}^{\text{PS-rich}} = 0.67$ . This indicates that the matrix phase in the LSCM images is actually a mixture of slow PS with some faster PMPS chains. On the other hand, for the symmetric (50/50) PS<sub>21</sub>/PMPS<sub>16</sub> blend, LSCM failed to detect any phase separation at ambient temperature. This result is again in agreement with the expectation born-out by the PS/PMPS phase diagram.<sup>[27]</sup>

### 3.2. Local Concentration Within the Domains

The LSCM images shown above do not have enough contrast to account for small amounts of fluorescently labeled PS that may be present within the PMPS phase. Below we will show that the technique of FCS when coupled with LSCM can provide additional information on the purity of phases in individual domains with submicrometer special resolution.

FCS is based on monitoring and recording the fluorescent intensity fluctuations caused by the diffusion of single fluorescent species through the focus of a confocal microscope. Autocorrelation analysis of these fluctuations yields the diffusion coefficient of the species, their concentration, and fluorescent brightness.<sup>[19]</sup> Ideally, one could apply FCS to study the diffusion of labeled PS chains within the PMPS-rich domains and infer the local concentration with sensitivity down to one PS chain per  $\mu\text{m}^3$ . However, performing such measurements is hindered by the very slow diffusion of the PS chains in the PMPS domains that leads to strong photobleaching and to further experimental problems. Alternatively, one can study the diffusion of very small tracers in the PMPS-rich domains and relate it to the local concentration within the domains. To enable this approach, a small amount of the fluorescent dye TDI was introduced as tracers in the PS<sub>116</sub>/PMPS<sub>16</sub> blend. The absorption maximum of TDI is around 630 nm, that is, far away from that of fluorescein ( $\approx 480$  nm) used for labeling the PS phase. Thus, the two dyes can be excited individually by different lasers and their fluorescence can be distinguished. The procedure was as follows: prior to the FCS measurement, the LSCM images were recorded using excitation at 488 nm (for fluorescein labeled PS). Then, the laser was focused in the center of a chosen PMPS domain and the excitation wavelength changed to 633 nm (for the TDI).

The time-dependent fluctuations of the fluorescent intensity caused by the diffusion of the TDI tracers through the focus were recorded. The corresponding autocorrelation curves yield the tracer diffusion time and diffusion coefficient. Subsequently, a new position was chosen within the PMPS-rich domain by moving the focus by 1  $\mu\text{m}$  away from the center and the autocorrelation curve was obtained. This procedure was repeated at 1  $\mu\text{m}$  increments from the center of the domain up to the domain boundaries. Measurements were performed in domains with diameters ranging from 3 to 20  $\mu\text{m}$ .

Typical results of the FCS measurements for the PS<sub>116</sub>/PMPS<sub>16</sub> blend first annealed at 120 °C for 24 h, quenched to ambient temperature, and measured after a period of  $\approx 2$  h are shown in Figure 2. The Figure depicts normalized autocorrelation curves of TDI corresponding at position 2 of the LSCM image. For comparison, the autocorrelation curve for the diffusion of the same dye in a PMPS homopolymer of the same molecular weight at ambient temperature is also shown. The figure further compares the diffusion times as a function of the measuring position within the PMPS grain. We can deduce that the TDI tracer is diffusing freely (according to the Fick's law) with nearly identical diffusion times in all cases. Thus, the results shown in Figure 2 indicate that the large dark domains are composed nearly exclusively by PMPS chains. This finding may sound paradoxical since it is the experience with polymer blends that one of the coexisting phase contain at least some amounts of the counter component. However, a closer inspection of the PS/PMPS phase diagram (Figure 1) reveals that at 25 °C the PMPS phase is exclusively composed from PMPS chains.

To explore further, this point a strongly asymmetric PS<sub>116</sub>/PMPS<sub>16</sub> blend was prepared (2/98) with the outlined procedure and imaged with LSCM. Even at this composition, phase-separated PS domains were clearly seen (Figure S3, Supporting Information) in accord with the phase diagram. In addition, the result is in excellent agreement with the local segmental relaxation of PMPS in the PS<sub>48</sub>/PMPS<sub>17</sub> symmetric blend investigated earlier with dielectric spectroscopy.<sup>[27]</sup> These results have shown that  $\phi_{\text{PMPS}}^{\text{PMPS-rich}} \approx 1.0$ , that is, a nearly pure PMPS phase. The reason for the different compositions in the two phases is that the PS glass temperature can intervene to the process of phase separation resulting in a hard component that cannot attain its equilibrium composition. On the other hand, the soft component (PMPS) can easily attain its equilibrium composition as observed experimentally.

With respect to Figure 2, it is only at the domain boundaries that the diffusion time increases by a factor of two suggesting mixing of PMPS chains with the slower PS chains. From these results, we deduce that the interfacial

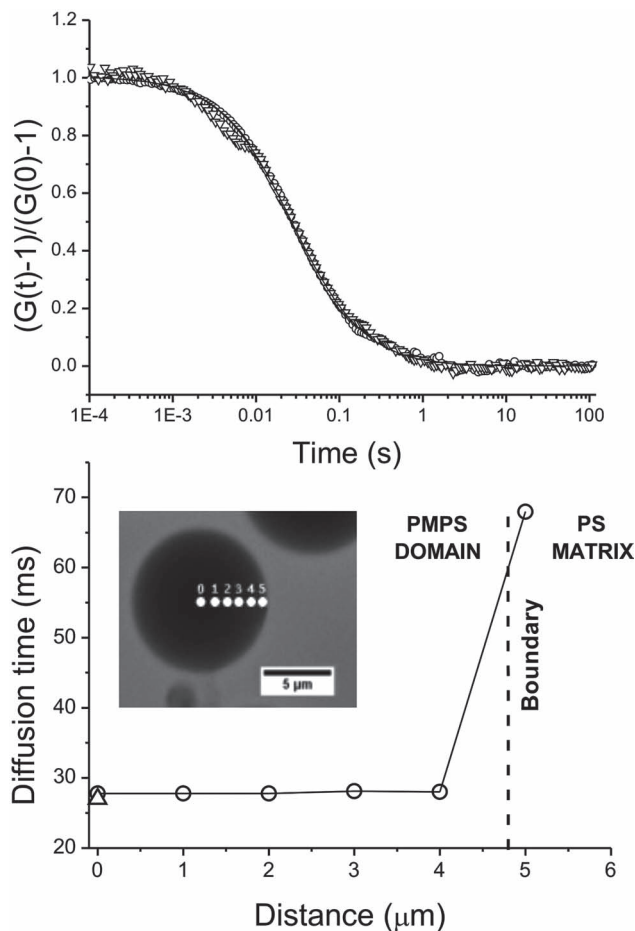


**Figure 2.** (Top) Normalized autocorrelation curves of terylene dye diffusing in bulk PMPS ( $\circ$ ) and within the PMPS domain ( $\Delta$ ) of the PS<sub>116</sub>/PMPS<sub>16</sub> blend. The blend was annealed at 120 °C for 24 h and then quenched at ambient temperature. The PMPS domain had a diameter of 10  $\mu\text{m}$  and the measurement refers to position 2 of the LSCM image) (Bottom) Diffusion times of terylene dye as a function of measuring position within the PMPS-rich domain of the LSCM image ( $\circ$ ). The diffusion time of the same dye in bulk PMPS ( $\Delta$ ) at the same temperature is also shown for comparison. The line is a guide to the eye.

width,  $\Delta$ , is smaller than  $\approx 0.5$   $\mu\text{m}$  and that the ratio  $2R/\Delta \gg 1$ , that is, consistent with the late stages of spinodal decomposition.

To test the sensitivity of FCS toward the purity of the PMPS domains, the same PS<sub>116</sub>/PMPS<sub>16</sub> blend was again annealed at 120 °C for 24 h and quenched at ambient temperature but then immediately investigated by FCS as a function of time. Under such conditions, the PMPS-rich phase may contain some slower PS chains. All measurements were made at the center of the domain and the result is shown in Figure 3. The figure depicts the reduction of the diffusion times toward the bulk PMPS value ( $\approx 27$  ms) as a result of the PS diffusion from the PMPS-rich domains towards the PS-rich domains.

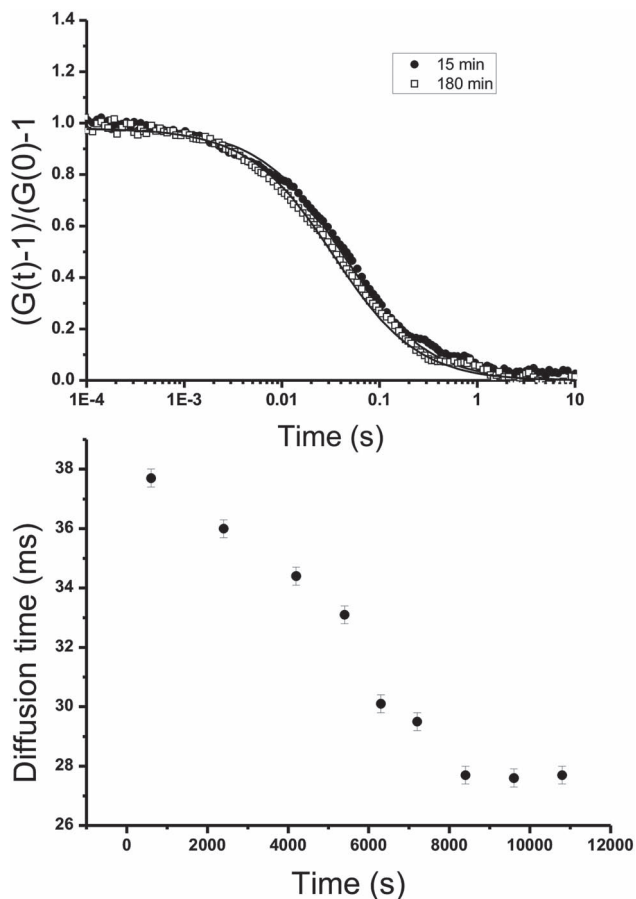


**Figure 3.** (Top) Normalized autocorrelation curves of terylene dye diffusing within the PMPS domain directly after quenching from 120 °C to room temperature (filled circles) and in the same PMPS domain after 3 h (empty squares) of the PS<sub>116</sub>/PMPS<sub>16</sub> blend. Measurements were made in the center of the domain. (Bottom) Diffusion times of terylene dye as a function of measuring time within the center of the PMPS-rich domain of the LSCM image.

## 4. Conclusion

The in situ investigation of the phase separation by LSCM was coupled with ex situ FCS measurements that provided both the dynamics of phase demixing and the purity of phases in a symmetric polymer blend. This combination demonstrated the possibility to obtain independent microscopic information on the local concentration within the phase-separated domains and further allowed estimating the interfacial width of a phase-separated blend by dynamic means. It would be of interest to explore the purity of phases for other blend compositions or in other blend systems that show bicontinuous phases instead. With respect to the latter a limiting factor is the size of the observation volume in FCS that is comparable to the size of the smaller grains ( $\approx 0.3 \mu\text{m}$ ).

## Supporting Information

Supporting Information is available from the Wiley Online Library or from the author.

**Acknowledgements:** We are thankful to Ronald P. White and Jane E.G. Lipson for providing the calculated phase diagram of the PS<sub>116</sub>/PMPS<sub>16</sub> blend investigated herein. This work was supported by DAAD (ID-50755038) and co-financed by the European Union (European Social Fund–ESF) and Greek national funds through the Operational Program “Education and Lifelong Learning” of the National Strategic Reference Framework (NSRF) – Research Funding Program: THALIS. Investing in knowledge society through the European Social Fund.

Received: May 9, 2012; Revised: May 24, 2012; Published online: July 3, 2012; DOI: 10.1002/marc.201200322

**Keywords:** fluorescence correlation spectroscopy; phase separation; polymer blends; purity of phases

- [1] (Ed: J. B. Pawley), *Handbook of Biological Confocal Microscopy*, Springer, New York **2006**.
- [2] S. R. Pygall, J. Whetstone, P. Timmins, C. D. Melia, *Adv. Drug Delivery Rev.* **2007**, *59*, 1434.
- [3] H. Verhooght, J. van Dam, A. P. J. de Boer, A. Draaijer, P. M. Houpt, *Polymer* **1993**, *34*, 1325.
- [4] H. Jinnai, Y. Nishikawa, T. Koga, T. Hashimoto, *Macromolecules* **1995**, *28*, 4782.
- [5] H. Jinnai, T. Hashimoto, D. Lee, S.-H. Chen, *Macromolecules* **1997**, *30*, 130.
- [6] C. R. López-Barrón, C. W. Macosko, *J. Microsc.* **2011**, *242*, 242.
- [7] J. R. Bell, K. Chang, C. R. López-Barrón, C. W. Macosko, D. C. Morse, *Macromolecules* **2010**, *43*, 5024.
- [8] T. Criszena, H.-J. Butt, K. Koynov, R. Simonutti, *R. Macromol. Rapid Commun.* **2012**, *33*, 114.
- [9] Q. Tran-Cong-Miyata, T. Kinohira, D.-T. Van-Pham, A. Hirose, T. Norisuye, H. Nakanishi, *Curr. Opin. Solid State Mater. Sci.* **2011**, *15*, 254.
- [10] L. Li, S. Sosnowski, C. E. Chaffey, S. T. Balke, M. A. Winnik, *Langmuir* **1994**, *10*, 2495.
- [11] N. Lören, A. Altskär, A.-M. Hermansson, *Macromolecules* **2001**, *34*, 8117.
- [12] S. Fransson, N. Lören, A. Altskär, A.-M. Hermansson, *Biomacromolecules* **2009**, *10*, 1446.
- [13] K. L. Liu, E. Widjaja, Y. Huang, X. W. Ng, S. C. J. Loo, F. Y. C. Boey, S. S. Venkatraman, *Mol. Pharmaceutics* **2011**, *8*, 2173.
- [14] K. Binder, P. Fratzl, *Phase Transformations in Materials* (Ed: G. Kostorz), Wiley-VCH, Weinheim, Germany **2001**.
- [15] T. Koga, K. Kawasaki, M. Takenaka, T. Hashimoto, *T. Physica A* **1993**, *198*, 473.
- [16] H. Tanaka, *J. Phys. Condens. Matter* **2000**, *12*, R207.
- [17] A. Shinozaki, Y. Oono, *Phys. Rev. Lett.* **1991**, *66*, 173.
- [18] I. M. Lifshitz, V. V. Slyozov, *J. Phys. Chem. Solids* **1961**, *19*, 35.
- [19] R. Rigler, E. S. Elsson, *Fluorescence Correlation Spectroscopy*, Springer-Verlag, New York **2001**.
- [20] T. Cherdhirankorn, G. Floudas, H.-J. Butt, K. Koynov, *Macromolecules* **2009**, *42*, 9183.
- [21] T. Cherdhirankorn, V. Harmandaris, A. Juhari, P. Voudouris, G. Fytas, K. Kremer, K. Koynov, *Macromolecules* **2009**, *42*, 4858.

- [22] A. Casoli, M. Schonhoff, *Biol. Chem.* **2001**, *382*, 363.
- [23] A. Best, T. Pakula, G. Fytas, *Macromolecules* **2005**, *38*, 4539.
- [24] M. Dorfschmid, K. Mullen, A. Zumbusch, D. Woll, *Macromolecules* **2010**, *43*, 6174.
- [25] K. Karatasos, G. Vlachos, D. Vlassopoulos, G. Fytas, G. Meier, A. Du Chesne, *J. Chem. Phys.* **1998**, *108*, 5997.
- [26] D. Vlassopoulos, A. Koumoutsakos, S. H. Anastasiadis, S. G. Hatzikiriakos, P. Englezos, *P. J. Rheol.* **1997**, *41*, 739.
- [27] A. Gitsas, G. Floudas, R. P. White, J. E. G. Lipson, *Macromolecules* **2009**, *42*, 5709.
- [28] B. Gerharz, T. Wagner, M. Ballauff, E. W. Fischer, *Polymer* **1992**, *33*, 3531.
- [29] F. Nolde, J. Q. Qu, C. Kohl, N. G. Pschirer, E. Reuther, K. Müllen, *Chem. Eur. J.* **2005**, *11*, 3959.
- [30] C. Jung, B. K. Müller, D. C. Lamb, F. Nolde, K. Müllen, C. Bräuchle, *C. J. Am. Chem. Soc.* **2006**, *128*, 5283.
- [31] J. E. G. Lipson, *Macromol. Theory Simul.* **1998**, *7*, 263.
- [32] R. P. White, J. E. G. Lipson, J. S. Higgins, *Macromolecules* **2012**, *45*, 1076.
- [33] A. Onuki, *J. Non-Cryst. Solids* **1994**, *172–174*, 1151.
- [34] P. Claudy, J. M. Letoffé, Y. Camberlain, J. P. Pascault, *Polym. Bull.* **1983**, *9*, 208.